

1-1-2013

# RF MEMS Reconfigurable Two-Band Antenna

A. Zohur

H. Mopidevi

D. Rodrigo

M. Unlu

L. Jofre

*See next page for additional authors*

---

## Recommended Citation

Zohur, A.; Mopidevi, H.; Rodrigo, D.; Unlu, M.; Jofre, L.; and Cetiner, Bedri A., "RF MEMS Reconfigurable Two-Band Antenna" (2013). *ECE Faculty Publications*. Paper 65.  
[http://digitalcommons.usu.edu/ece\\_facpub/65](http://digitalcommons.usu.edu/ece_facpub/65)

This Article is brought to you for free and open access by the Electrical and Computer Engineering, Department of at DigitalCommons@USU. It has been accepted for inclusion in ECE Faculty Publications by an authorized administrator of DigitalCommons@USU. For more information, please contact [becky.thoms@usu.edu](mailto:becky.thoms@usu.edu).



---

**Authors**

A. Zohur, H. Mopidevi, D. Rodrigo, M. Unlu, L. Jofre, and Bedri A. Cetiner

# RF MEMS reconfigurable two-band antenna

A. Zohur, H. Mopidevi, *Student Member, IEEE*, D. Rodrigo, *Student Member, IEEE*, M. Unlu, L. Jofre, *Fellow, IEEE*, and B. A. Cetiner, *Member, IEEE*

**Abstract**— The design methodology, analysis, and characterization of a Radio Frequency MicroElectroMechanical Systems (RF MEMS) based reconfigurable antenna operating in the United States Public Safety bands are presented. It has two modes of operation with central frequencies of 718 and 4960 MHz, providing a high reconfigurable frequency ratio of  $\sim 7$ . This antenna is electrically small with lateral dimensions being  $\sim \lambda/10 \times \lambda/10$  at 718 MHz. The reconfigurability between the modes is achieved by a single RF MEMS switch, which enables changing the length of the current flow path, thereby the resonance frequency is changed. The measurement results for impedance and radiation characteristics of the fabricated antenna prototype agree well with the simulations. The measured bandwidths of the antenna are 2.6% and 7.6% at 718 MHz and 4960 MHz, respectively.

**Index Terms**— Frequency reconfigurable antennas, UHF antennas, Electrically small antennas, Antenna measurements, Antenna radiation patterns

## I. INTRODUCTION

Interoperability between widely spaced frequency bands enhances the effectiveness of a multi-mode multi-band wireless communication system in improving the quality of communication. This type of robust communication is also critical when a large number of emergency responders (public safety (PS) personnel: police, firefighters, and emergency medical services) operating over different bands need to be accommodated to deal with man-made or natural catastrophic situations. For a single antenna to be able to cover multiple frequency bands, various design approaches are used – multi-frequency antenna covering each individual band [1], a broadband antenna covering the entire frequency bandwidth (BW) [2], or a frequency reconfigurable antenna (FRA) with a narrow instantaneous operating BW that can be tuned over the entire band [3]. When the frequency bands of operation are widely separated, it is difficult to provide a good impedance match in a multi-frequency antenna at such distant resonances. Moreover, when the tradeoff between the separation of frequency bands and the maintenance of the integrity of radiation characteristics over the bands is considered, among the three approaches, the reconfiguration approach provides an

optimum solution.

Planar inverted F-antennas (PIFAs) [4] are commonly used in mobile devices, where compact antennas are required. With the advantages brought by the RF MEMS technology [5], a MEMS integrated frequency reconfigurable PIFA would therefore become highly essential for emergency responders to have effective wireless communications. In this paper, an FRA, which can reconfigure its frequency of operation between two widely spaced United States (US) PS bands (700 MHz and 4900 MHz), while at the same time maintaining a reasonable integrity in its radiation characteristics, is reported. The reconfigurability is achieved by using a single RF MEMS ohmic contact switch [6], which is integrated at a strategic location of the antenna geometry (see fig. 1). The switch is used to change the path length of the current on the antenna. This, in turn, enables the antenna to reconfigure its operating frequency band with one of the two central frequencies of 718 MHz and 4960 MHz with a frequency ratio of  $\sim 7$ .

The design of an FRA requires additional design constraints as compared to an antenna with fixed properties. The key aspect of this design methodology is to maintain the desired performance characteristics of the FRA in one mode of the operation while optimizing the parameters of the other mode of operation. In other words, the desired performance characteristics and the associated physical parameters of both modes of operation (700 MHz and 4900 MHz) need to be jointly optimized. The reconfigurable antenna presented in this paper is electrically small (lateral dimensions  $\sim \lambda/10 \times \lambda/10$  at 718 MHz) and accomplishes a high reconfigurable frequency ratio when compared to similar MEMS integrated FRAs in the literature [7, 8]. The working mechanism of this antenna may be explained by considering its hybrid structure between a two arm asymmetric dipole (partially unbalanced structure) and a PIFA (unbalanced structure), as explained in Section II.A. Measured and simulated radiation patterns and reflection coefficients of the antenna, with a good agreement between them, are also presented.

## II. ANTENNA DESIGN, OPERATION, AND ANALYSIS

The pictures and schematics of the proposed antenna are shown in fig. 1a and fig. 1b. It is composed of two layers that are fabricated on RO4003 substrate ( $\epsilon_r = 3.38$ ,  $\tan \delta = 0.002$ ), and air is used as the substrate between the two layers. The bottom layer, which also contains the RF MEMS switch, is used as the reconfigurable metal layer (see fig. 1a), and the top layer is used for the top patch (see fig. 1b). The antenna has two modes of operation that are centered around 718 MHz (Mode 1) and 4960 MHz (Mode 2). When the meander (indicated as Mode 1 meander in fig. 1a) is connected (switch

---

Manuscript received December 15, 2012. This work was supported in part by the Center of Excellence Program of the Utah Governor's Office and by the United States Department of Justice with Award No. 2009-SQ-B9-K005 awarded by the National Institute of Justice, Office of Justice Programs.

A. Zohur, H. Mopidevi, M. Unlu, and B. A. Cetiner are with the department of Electrical and Computer Engineering, Utah State University, Logan, UT 84322-4120 USA (e-mail: bedri.cetiner@usu.edu)

D. Rodrigo and L. Jofre are with the Universitat Politècnica de Catalunya, Barcelona 08034, Spain (e-mail: luis.jofre@upc.edu).

is ON) the antenna operates in Mode 1, and when it is disconnected (switch is OFF) the antenna operates in Mode 2. The distance between the two layers is optimized to be 5.5 mm. To accommodate the capacitive feed (shown in fig. 1b) in the design, which compensates for the inductance effect of the coaxial feed, a RO4003 substrate with a thickness of 0.813 mm is sandwiched by the bottom conductive plate of the capacitive feed and top patch metal of the antenna.

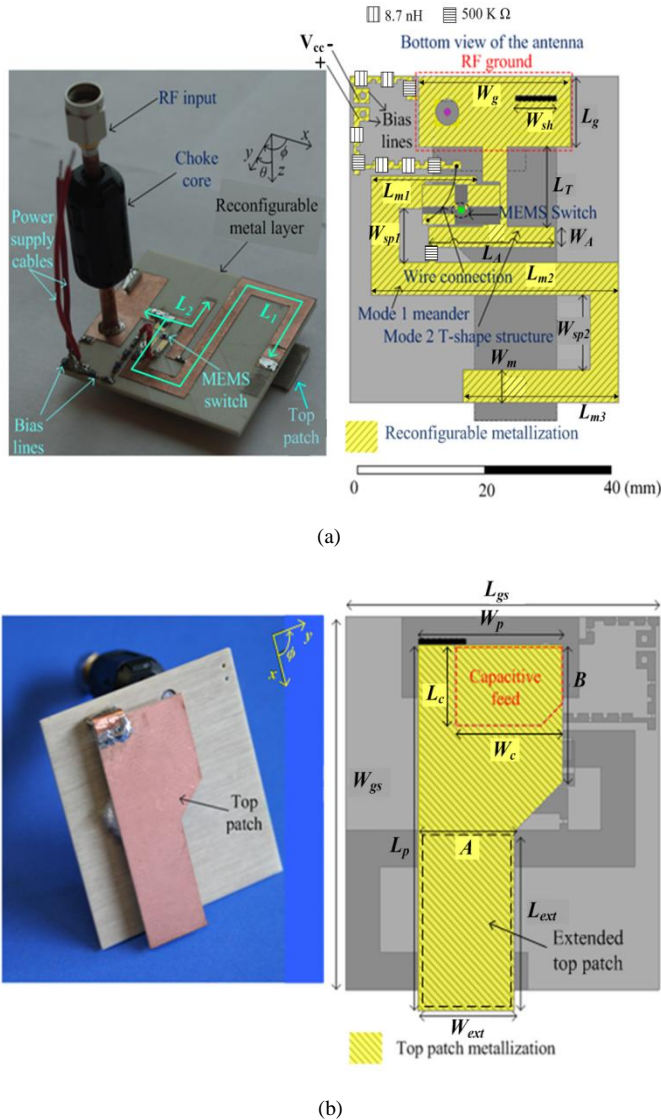


Fig.1. The photographs and schematics of the RF MEMS integrated antenna depicting the critical design parameters: (a) bottom view ( $L_1 \sim 104$  mm and  $L_2 \sim 19$  mm) (b) top view

**A. Design Methodology**

ANSYS HFSS v13 [9] was used to carry out numerical analyses for the design. Initially, it is designed to satisfy the requirements of Mode 2, where T-shaped structure [10], tapering of the patch [11], and capacitive feeding techniques [2, 12] are employed in order to increase the BW. Then, a meander (Mode 1 meander in fig.1a) is introduced to reduce the resonance frequency of the antenna to 718 MHz (Mode 1). The length, shape, and position of the meander are important for proper operation of the antenna. Although the meander

reduces the resonance frequency significantly, it does not give a good reflection coefficient at Mode 1, if not optimized jointly with other critical design parameters such as the dimensions of top patch ( $L_p$ ,  $W_p$ ,  $A$ ,  $B$ ,  $L_{ext}$ , and  $W_{ext}$ ) shown in fig. 1. Therefore, the antenna has been re-optimized by extending the top patch metallization (using parameters  $L_{ext}$  and  $W_{ext}$ ) so that a good reflection coefficient in each mode of operation can be achieved.

**B. Analysis and operation**

In this design, the Mode 1 meander ( $L_1$ ) and Mode 2 T-shape ( $L_2$ ) structures combined with the top patch are the radiating structures (in Modes 1 and 2 respectively), and the top patch (especially width  $W_{ext}$ ) is useful in providing a good reflection coefficient (matching condition) for each mode of operation. This explanation is supported by the simulated surface current plots shown in fig. 2 where the two arm asymmetric dipole behavior (with currents distributed along the two arms) may be mainly identified for the Mode 1 and the PIFA character (with a strong current into the upper active patch) may be mainly seen for the Mode 2. The parameters  $L_1$  ( $\sim 104$  mm) and  $L_2$  ( $\sim 19$  mm), shown in fig 2, correspond to approximately  $\lambda/4$  resonant lengths at  $\sim 700$  MHz and  $\sim 4.9$  GHz, respectively. The reduced RF ground shown in fig. 1a may be seen as a small common ground for both modes of operation. In order to compensate for the limited size of the ground plane when connected to a coaxial transmission line a choke balun has been added. For real operation on portable and hand-held public safety devices the two arm asymmetric dipole character may prevail and the need for a balancing balun is reduced.

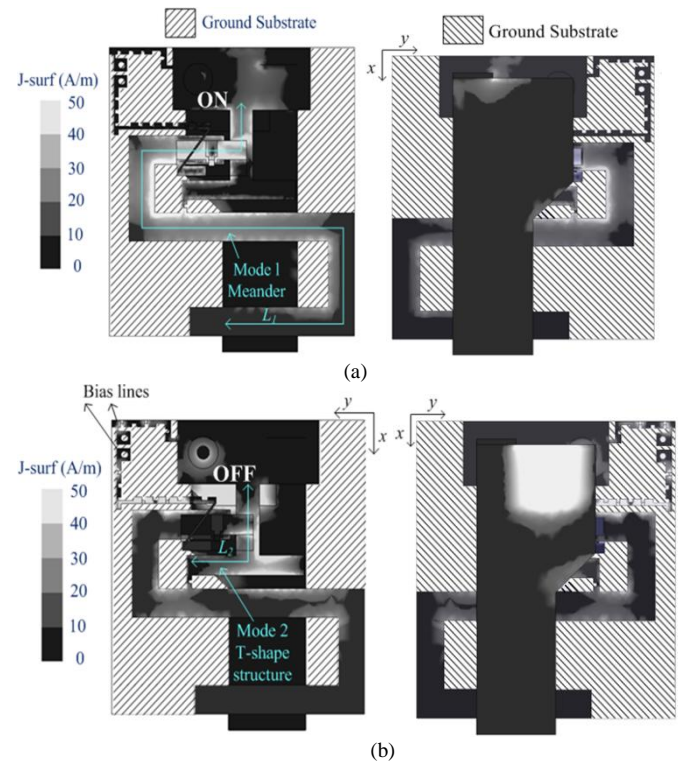


Fig.2 Simulated surface current plot of the antenna along with the status of MEMS switch in (a) Mode 1 and (b) Mode 2

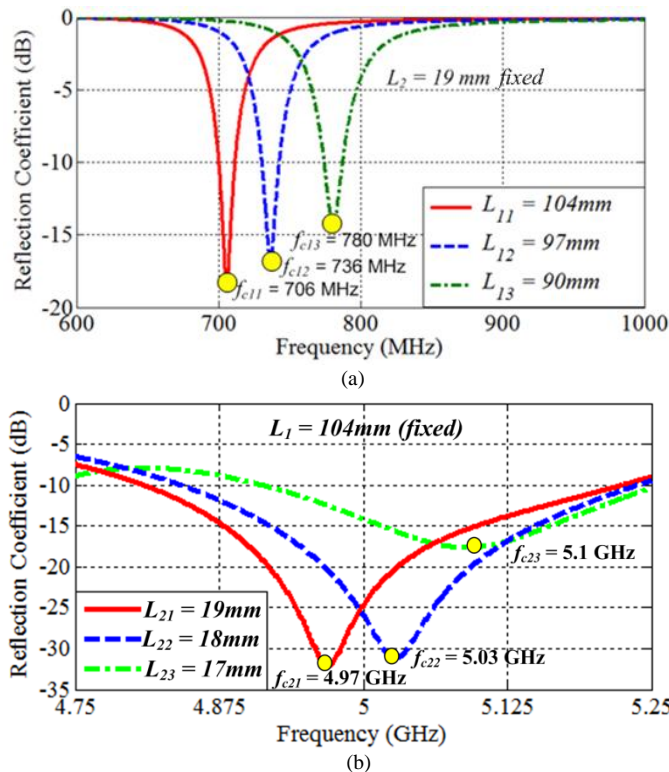


Fig.3 Effect of change in parameters (a)  $L_1$  in Mode 1 and (b)  $L_2$  in Mode 2

To further explain the working mechanism of the antenna, the effect of parameters  $L_1$  and  $L_2$  on the antenna's reflection coefficient in Mode 1 and Mode 2, respectively, was studied. As shown in fig. 3a, when  $L_2$  was kept (=19mm) fixed, change in the parameter  $L_1$  resulted in a shift in the resonant frequency  $f_{c1}$  of Mode 1, with  $L_{11}$ (=104mm),  $L_{12}$ (=97mm), and  $L_{13}$ (=90mm) being  $\sim \lambda/4$  resonant lengths at  $f_{c11}$ (=706MHz),  $f_{c12}$ (=736MHz), and  $f_{c13}$ (=780MHz), respectively. Similarly, while  $L_1$  was kept (=104mm) fixed, change in the parameter  $L_2$  resulted in a shift in the center frequency  $f_{c2}$  of Mode 2, as shown in fig. 3b. Although the exact  $\lambda/4$  resonant lengths at  $f_{c21}$ (=4.97GHz),  $f_{c22}$ (=5.03GHz), and  $f_{c23}$ (=5.1GHz) are equal to 15.1mm, 14.9mm, and 14.7mm respectively the effective resonant lengths obtained from simulations are  $L_{21}$ (=19mm),  $L_{22}$ (=18mm), and  $L_{23}$ (=17mm), respectively. This is mainly due to the extended top patch coupling EM energy to the disconnected Mode 1 meander, which thereby parasitically loads the Mode 2 T-shape structure, due to its close proximity.

Table 1. The critical design parameters of the antenna (all dimensions are in mm)

$W_{gs}$	45	$W_{ext}$	12.8	$L_g$	9.8	$W_{sp1}$	7.5
$L_{gs}$	41.8	A	12.8	$L_T$	11	$W_{sp2}$	10.3
$W_p$	19.2	B	16.5	$W_A$	3.9	$W_m$	4.5
$L_p$	44	$L_c$	9.6	$L_A$	18.5	$W_{sh}$	6.4
$L_{ext}$	21.6	$W_c$	14.4	$L_1$	104	$L_2$	19
$W_g$	23.5	$L_{m1}$	16.4	$L_{m2}$	38.6	$L_{m3}$	24.2

The critical design parameters for the antenna are presented in fig. 1 and listed in Table 1. The OFF state capacitance and

ON state resistance of the RF MEMS switch are also taken into account during the design, which have significant effect on the values of the design parameters. The switch was modeled using impedance boundary conditions in HFSS [9]. The typical off state capacitance (=30 fF) and on state resistance (=1 Ohm) of MEMS device were used to model the equivalent sheet reactance and resistance respectively. Another important part of the design is the compensation of the effects of copper bias lines (see fig. 1a) used to actuate the RF MEMS switch. The two bias lines are delimited by a total of 5 SMD inductors (8 nH) and 3 SMD resistors (500 k $\Omega$ ) (see fig. 1a) so that the bias lines have negligible effects on the antenna characteristics in both modes of operation.

### III. MEASUREMENT RESULTS AND DISCUSSION

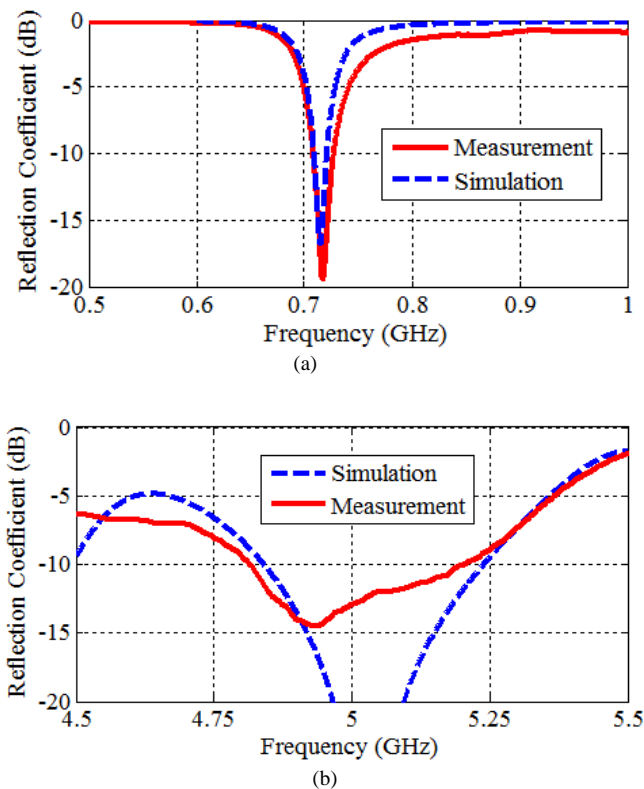


Fig.4. Simulated and measured reflection coefficients of the antenna in (a) Mode 1 (b) Mode 2

The reflection coefficient of the antenna is measured using Agilent 8722ES network analyzer with one-port Short Open Load (SOL) calibration. During the measurements,  $V_{cc} = 90V$  actuation voltage is used for the RF MEMS switch actuation. A high actuation voltage of 90 V is a disadvantage of MEMS switch technology over the semiconductor switch technologies, i.e., pin-diode or FET. However, MEMS has some important advantages as well:

1. While a typical pin diode draws several mA of current a MEMS switch draws negligible amount of current in nano amperes which results in exceedingly less power consumption.
2. Insertion loss and isolation characteristics of MEMS switches over the entire frequency of operation (700 MHz to 4900 MHz) are much better than a pin diode or FET

3. Although it was not applied in this structure, MEMS has the advantage of being monolithically integrated, which is not possible for a pin diode or FET.

Fig. 4a and fig. 4b show the reflection coefficient measurement results of the fabricated antenna prototype in both modes, which agree reasonably well with the simulations. The measurement results show that the antenna has a 10-dB bandwidth of 20 MHz (2.6%) and 223 MHz (7.6%) in Mode 1 and Mode 2, respectively.

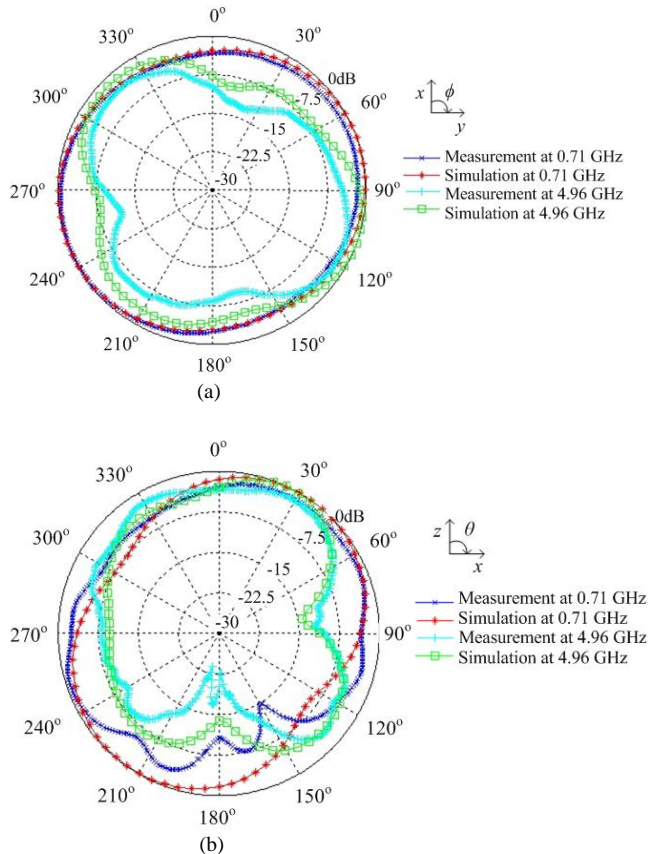


Fig. 5. Simulated and measured total normalized electric field intensities of the antenna in (a)  $xz$  plane (b)  $xy$  plane

To obtain the radiation patterns, the antenna prototype is placed on a rotor in the anechoic chamber and a power supply was used to actuate the single MEMS switch. The total normalized electric field intensities in  $xz$  and  $xy$  planes are shown in fig. 5a and fig. 5b. As seen from these figures, the measured and simulated radiation patterns agree reasonably well. A dipole type radiation pattern is expected from the geometry of the main radiating elements – Mode 1 meander and Mode 2 T-shape structures in Modes 1 and 2 respectively. Correspondingly, a figure of eight pattern in the  $xz$  plane, in both modes of operation (see fig. 5a), confirms the analysis. The null in the radiation pattern of Mode 2 in  $\theta = 180^\circ$  direction (in fig. 5a) and the compromise of radiation pattern integrity in  $xy$  plane between both modes of operation (in fig. 5b) is mainly due to the effect of extended top patch on Mode 2 operation as explained in Section II. The differences between simulations and measurements may mainly be attributed to the obstruction of the rotor in measurement in  $\theta =$

$180^\circ$  direction and, the undesired radiation of the power supply cables (see fig. 1a). The measured directivities of the antenna obtained by integration of the 3D patterns are 2.44 dB at 710 MHz (Mode 1) and 4.01 dB at 4960 MHz (Mode 2) which are quite close to the simulated results. The antenna efficiency has been measured using Wheeler's cap method. The measured efficiency is 75% at 710MHz (Mode 1) and 85% at 4960 MHz (Mode 2), leading to gains of 1.2dB and 3.3dB, respectively. The variation of efficiency with respect to frequency bandwidth for both modes of operations stays relatively constant as observed from measurements and simulations.

#### IV. CONCLUSION

A frequency reconfigurable electrically-small antenna with a high reconfigurable frequency ratio of  $\sim 7$ , between two frequency bands (718 MHz and 4960 MHz), is presented for US Public Safety wireless communications. The reconfigurability is obtained using a single RF MEMS switch. Both modes of operation are jointly optimized and the impedance and radiation pattern measurements are characterized. The fabricated antenna shows good measured performances, which agree reasonably well with the simulations. The antenna achieves a reasonably wide measured bandwidth of 2.6% at 718MHz given its electrically-small lateral dimensions of  $\sim \lambda/10 \times \lambda/10$ . The integrity of radiation patterns is also reasonably maintained in both modes of operation. Work is under way to further improve the radiation integrity over the reconfigurable modes of operation.

#### REFERENCES

- [1] Jin-Sen Chen, "Multi-frequency characteristics of annular-ring slot antennas," *Microwave and Optical Technology Letters*, Vol. 38, No. 6, Sept. 2003.
- [2] Mopidevi, H.; Rodrigo, D.; Kaynar, O.; Jofre, L.; Cetiner, B.A.; , "Compact and Broadband Antenna for LTE and Public Safety Applications," *Antennas and Wireless Propagation Letters, IEEE* , vol.10, no., pp.1224-1227, 2011.
- [3] B. A. Cetiner, G.R. Crusats, L. Jofre, and N. Biyikli, "RF MEMS Integrated Frequency Reconfigurable Annular Slot Antenna," *Antennas and Propagation, IEEE Transactions on* , vol.58, no.3, pp.626-632, March 2010.
- [4] K. Hirasawa, and M. Haneishi, *Analysis, design, and measurement of small low profile antennas*. Norwood, MA, USA: Artech House, 1993.
- [5] G.M. Rebeiz, *RF MEMS Theory, Design, and Technology*. John Wiley & Sons Inc., Hoboken, NJ, 2003.
- [6] Radant MEMS, 255 Hudson Road, Stow, MA 01775.
- [7] K. R. Boyle, and P.G. Steeneken, "A Five-Band Reconfigurable PIFA for Mobile Phones," *Antennas and Propagation, IEEE Transactions on* , vol.55, no.11, pp.3300-3309, Nov. 2007
- [8] P. Panaia, C. Luxey, G. Jacquemod, R. Staraj, G. Kossivas, L. Dussopt, F. Vacherand, and C. Billard, "MEMS-based reconfigurable antennas," *Industrial Electronics, 2004 IEEE International Symposium on* , vol.1, no., pp. 175- 179 vol. 1, 4-7 May 2004
- [9] ANSYS HFSS, version 13.0, build: July 18 2007, Ansoft Corporation, <http://www.ansoft.com>
- [10] F. Wang, Z. Du, Q. Wang, and K. Gong, "Enhanced-bandwidth PIFA with T-shaped ground plane," *Electronics Letters*, Vol.40, no.23, pp. 1504- 1505, 11 Nov. 2004.
- [11] C. K. Byung, D. P. Ju, and D. C. Hyung, "Tapered type PIFA design for mobile phones at 1800 MHz," *Vehicular Technology Conf.*, Orlando, FL, USA, Vol. 2, pp. 1012-1014, 2003.
- [12] G.A.E. Vandebosch, "Capacitive matching of microstrip antennas", *Electron. Letter*, 1995, 31, (18), pp. 1535-1536.